



Removal of boron from water by batch adsorption onto bovine bone char: optimization, kinetics and equilibrium

S. A. Valverde¹ · J. C. V. Azevedo¹ · A. B. França¹ · I. J. B. Santos¹ · F. L. Naves¹ · P. L. Mesquita¹

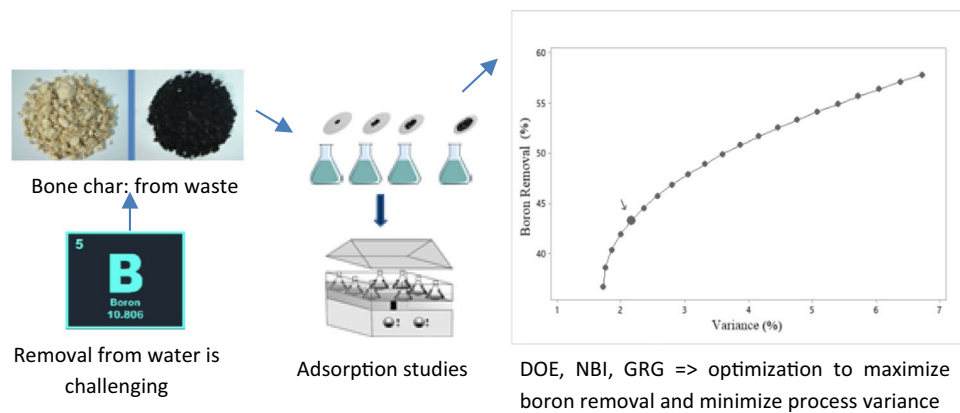
Received: 11 July 2022 / Revised: 18 September 2022 / Accepted: 29 October 2022 / Published online: 19 November 2022

© The Author(s) under exclusive licence to Iranian Society of Environmentalists (IRSEN) and Science and Research Branch, Islamic Azad University 2022

Abstract

With the widespread of boron application, more and more boron residues pollute water sources, leading to a series of environmental and health problems. In this context, the objective of this work was to investigate boron adsorption and to set the optimal conditions to maximize boron uptake from water by bone char (a low cost material produced from bovine bones waste) and, simultaneously, to minimize the variance of the process, aiming at future industrial applications. Design of experiments was carried out using the central composite design. Optimization was carried out by generalized reduced gradient and normal border intersection methods. At initial effluent pH of 7.72, solid–liquid ratio of 59.95 g L⁻¹ and an initial boron concentration of 18.63 mg L⁻¹, it was possible to reach 43% of boron removal, with a variance of 2%. The equilibrium study showed that Freundlich model described better the system, compared to Langmuir, Henry, Temkin and Langmuir–Freundlich isotherms, suggesting a reversible process. Pseudo-second-order adsorption kinetics model best fitted experimental data.

Graphical Abstract



Keywords Boron · Adsorption · Bovine bone char, water

Editorial responsibility: Chongqing Wang.

✉ P. L. Mesquita
patriciamesquita@ufsj.edu.br

¹ Postgraduate Program in Chemical Engineering,
Universidade Federal de São João del-Rei – Campus Alto
Paraopeba, Rodovia MG 443, km07, Fazenda Do Cadete,
Ouro Branco, MG 36497-899, Brazil

Introduction

Boron (B) is an element distributed vastly in the hydrosphere and lithosphere on earth in forms of boric acid, borate salts, and borosilicate minerals (Guan et al. 2016; Dolati et al. 2017). These compounds are commonly used as an antiseptic, bactericide, cleaning agent, such as in soaps and detergents, fire retardants, fertilizers, insecticides and herbicides. Boron is also used in many industrial applications, including



the production of glass, porcelain, ceramic, semiconductors and metal alloys (Alkurdi et al. 2019).

The main sources of boron can be either natural such as leaching from rocks, soils containing borates and borosilicates, and volcanic activities, or industrial (Goren and Okten 2021). With the increase in the consumption boron compounds in industry and agriculture over the last two decades, and subsequent disposal into the environment, the concentration of this element in some water resources has also enhanced, becoming a serious threat to ecological systems, humans, animals and plants (Jalali et al. 2016; Yan et al. 2022).

Although boron is an essential micronutrient, excessive exposure can cause detrimental effects to plants, animals, and humans (Zhang et al. 2022). For some plant species, boron is the element with the narrowest range between deficiency and toxicity, being considered an essential nutrient in low concentrations (up to 0.3 mg L^{-1}), and toxic in concentrations slightly higher than 0.5 to 2.4 mg L^{-1} (Brdar-Jokanović 2020). In contact with certain level of boron, plants may exhibit symptoms such as chlorosis and necrosis in the leaves, decreased growth, inhibition of photosynthesis and, eventually, death (Xin and Huang 2017).

Although boron toxicity is more pronounced in plants, in humans, prolonged use of water containing this agent may cause gastrointestinal problems, circulatory dysfunction, blood circulation disorders and problems in the reproductive system, including infertility, fetal malformation and dysplasia (Dolati et al. 2017; Wang et al. 2018). Therefore, the maximum concentration of boron in drinking water has been regulated in some countries and regions, for example, the European Union recommends 1.0 mg L^{-1} and the World Health Organization (WHO) 2.4 mg L^{-1} (EU 1998; WHO 2017).

Consequently, several technologies have been studied for removing boron from aqueous solutions in the last decade, including: adsorption (Delazare et al. 2014; Jalali et al. 2016; Lyu et al. 2017; Demey et al. 2019; Heredia et al. 2019), reverse osmosis (RO) (Chen et al. 2016; Wang et al. 2018), ion exchange (Kameda et al. 2017), electrocoagulation and electrodialysis (Dolati et al. 2017; Chen et al. 2020), coagulation and chemical precipitation (Yoshikawa et al. 2012; Sasaki et al. 2016; Chorghé et al. 2017), phytoremediation with native plants known as boron hyperaccumulators and hypertolerants (Chen et al. 2017; Türker et al. 2017; Xin and Huang 2017) and hybrid processes (Oladipo and Gazi 2016; Ban et al. 2019).

Among them, adsorption is considered the most promising method, due to its low cost, operational simplicity, regeneration capacity depending on the adsorbent adopted and, in general, it is effective in aqueous media, even for low concentration of this contaminant (Lyu et al. 2017). In recent years, several types of adsorbents have been studied

to remove boron from aqueous solutions, including resins and chelating fibers, activated carbon, clays and minerals, metal oxides, industrial waste materials, natural materials and metal–organic frameworks (Lin et al. 2021).

The use of adsorbents derived from agricultural residues and low added value solids has shown great potential in the removal of boron from effluents due to the presence of a highly porous structure, several functional groups and low production cost (Yagmur Goren et al. 2022). Kehal et al. (2010) used vermiculite modified by thermal shock for boron removal in effluents achieving an adsorption capacity of 0.16 mg g^{-1} . Jaouadi (2021) prepared an activated carbon from pine sawdust for the treatment of boron in water and reported an adsorption capacity of 1.58 mg g^{-1} . Melliti et al. (2020) reported that activated carbon from palm bark was used for the removal of boron from the aqueous medium and found an adsorption capacity of 2.37 mg g^{-1} .

Bovine bone char has already been applied for water and wastewater treatment, including color removal (Ip et al. 2010; Reynel-Avila et al. 2016; Cheng et al. 2017; Cruz et al. 2019); removal of metals, such as chromium (Isaacs-Paez et al. 2014), arsenic (Alkurdi et al. 2021), copper and zinc (Hernández-Hernández et al. 2017), as well as for water defluoridation (Rojas-Mayorga et al. 2015; Medellín-Castillo et al. 2016; Nigri et al. 2016b; Asgari et al. 2019) and removal of organic compounds (Mesquita et al. 2017a; Mendes et al. 2019; Nigri et al. 2019). In addition to its low cost, adsorption studies with bone char have evaluated its ability to regenerate (Medellín-Castillo et al. 2016; Nigri et al. 2016a, b; Mesquita et al. 2017a, b; Meili et al. 2019). The use in multiple cycles, thus increasing its life and consequently, reduces the process costs and the unwanted generation of residues (Nigri et al. 2016a). Besides, bovine bone char composes a sustainable cycle since, in addition to being produced from voluminous residues, after its use and depletion in the adsorption process, it could be reused as a renewable and efficient phosphate fertilizer for deficient soils (El-Refaey et al. 2015). Indeed, the addition of this material to the soil may improve physical and chemical characteristics while also implying in significantly reduced emissions of carbon dioxide (CO_2) and other greenhouse gases into the atmosphere (Saleh et al. 2020).

Sasaki et al. (2016) investigated the co-precipitation of borate with hydroxyapatite (HAp, $(\text{Ca}_{10}(\text{PO}_4)_6(\text{OH})_2)$) using $\text{Ca}(\text{OH})_2$ as a mineralizer in the presence of phosphate. The authors suggested that the borate removal process consisted of, at least, two steps: (1) simultaneous immobilization of borate with precipitation of HAp (co-precipitation), where borate was immobilized together with phosphate in the crystallization of HAp and (2) immobilization through sorption in precipitated HAp (Sasaki et al. 2016).

Thus, the present work proposed the use of bovine bone char, a low cost material, produced from food industry,

slaughterhouse and tanneries waste, as a potential adsorbent for boron uptake, since it is mainly composed of calcium phosphate, as hydroxyapatite, calcium carbonate (calcite) and only 10% (weight) of carbon (Mesquita et al. 2017a). Therefore, even though boron removal is still seen as a challenge, this work is a new contribution to better understand the adsorption process of this contaminant onto bovine bone char, mainly regarding kinetics, equilibrium and optimization of process conditions to support future decisions on industrial scaling up.

Material and methods

Materials and samples for adsorption tests

Bone char

Bovine bone char was produced by calcination in an oven with limited amount of oxygen, at a temperature of 800 °C, for 8 h, by Bonechar Carvão Ativado Ltda., in Maringá, Paraná, Brazil (Mendes et al. 2019). Quartering was performed according to Brazilian technical standards for reducing field samples for laboratory tests (ABNT NBR NM 27: 2001; ABNT, 2001). Sieving was carried out by vibrating sieves of 6, 12, 32, 48, 60 and 100 mesh (Bertel Indústria Metalúrgica—Ltda.), for 15 min at 5 rpm, and particles of 12–32 mesh (0.5–1.4 mm) of bovine bone char was selected for the adsorption tests. To guarantee the removal of fines that could be adhered to the surface, the material was washed 4 times with distilled water (250 g of bone char/ L of water) and dried in an oven (Sterilifer SX1.1 DTME) at 120 °C for 2 h (Mesquita et al. 2017a).

Steam pre-treatment of bovine bone char The methodology for the steam pre-treatment was based on Mesquita et al (2018). The assembly set up consisted of a glass tube in which cotton supported a 60 cm deep bone char bed. A rubber hose connected the open bottom of the glass tube to a 500 mL Kitasato flask, containing water, which was kept on a hot plate, under stirring, at 200.0 ± 1.0 °C. The steam produced was at 96.0 ± 0.5 °C and the contact time with the char was 15 min.

Synthetic effluent

The synthetic effluent at 18.63 mgB L^{-1} was prepared by dissolving 0.63 g of ROLLIT EZ505 deoxidizer (50–70% disodium tetraborate pentahydrate ($\text{Na}_2\text{B}_4\text{O}_7 \cdot 5\text{H}_2\text{O}$), Budenheim México SA), in 1 L of distilled water, under stirring. The pH of the solution (9.0) was measured with a pH meter Digimed—22 and corrected using 0.1 mol L^{-1} of sodium hydroxide, NaOH (Cromato Produtos Químicos Ltda.), or

0.1 mol L^{-1} nitric acid, HNO_2 (Dinâmica Ltda.) solutions, as defined in the design of the experiment (Sect. 2.4.1).

To assess the influence of the initial boron concentration, effluent solutions were prepared in concentrations of 4.9; 10.8; 20.4; 29.5 and 38.0 mg L^{-1} , using the same reagents.

Adsorbent characterization

Surface area and pore size distribution were carried out based on nitrogen adsorption/desorption Brunauer–Emmet–Teller (BET) multipoint analysis and Barret–Joyner–Halenda (BJH) model, respectively (Quantachrome equipment, model Nova 1000e). N_2 as inert gas, 100 °C preparation temperature, under vacuum, for 6 h.

X-ray diffraction (XRD) to identify crystalline phases in the adsorbent was also performed according to the powder or Debye Scherrer method, in a Rigaku diffractometer (Miniflex 600) operating with $\text{CuK}\alpha$ radiation, goniometer speed $0.5^\circ \text{ min}^{-1}$, angle range from 5° to 80° (2θ) (Mesquita et al. 2017a).

Fourier transform infrared spectrometry (FTIR) analyses for new and boron saturated bovine bone char were carried out in a Bruker Alpha II equipment (resolution 4 cm^{-1} , range from 400 to 4000 cm^{-1}). Attenuated Total Reflectance (ATR) diamond crystal methodology was used, with 128 scans.

Zeta potential and mean hydrodynamic diameter were determined according to D'Onofre Couto et al. (2021) by photon correlation spectroscopy at 25.0 ± 0.1 °C (Zetasizer Nano ZS, Malvern Instruments Inc.).

Points of zero charge (PZC) pH of bone chars were carried out according to the “experiment of 11 points” methodology, described by Regalbuto and Robles (2004). 50 mg of the adsorbent and 50 mL of aqueous solution were mixed under 11 different initial pH conditions (2, 3, 4, 5, 6, 7, 8, 9, 10, 11, 12), corrected with HCl or NaOH solutions, 0.1 mol L^{-1} , and the pH, after 24 h of equilibrium, was measured again. The pH_{PZC} was obtained from the arithmetic mean of the points that tend to the same value.

Adsorption experiments

All batch adsorption tests were carried out in an orbital shaker (New Technique-712), at 180 ± 1 rpm and controlled temperature as designed for each study. According to the solid–liquid ratio desired, the bone char masses were weighed on an analytical scale (Mars-AY220) and added to 100 ml of effluent in a 250 ml erlenmeyer flask. After equilibrium time was achieved, the treated effluent and the bovine bone char were filtered through $8 \mu\text{m}$ quantitative filter paper. The bone char was dried in a laboratory oven at 50 °C for 24 h.



Table 1 Non-randomized CCD generated tests for boron adsorption onto bovine bone char

Experiment	Initial effluent pH*	Solid–liquid ratio (g L ⁻¹)	Boron initial concentration (C ₀) (mg L ⁻¹)
<i>“In natura” bone char</i>			
1	5.0	20.0	10.8
2	11.0	20.0	10.8
3	5.0	80.0	10.8
4	11.0	80.0	10.8
5	5.0	20.0	29.5
6	11.0	20.0	29.5
7	5.0	80.0	29.5
8	11.0	80.0	29.5
9	8.0	50.0	20.4
10	8.0	50.0	20.4
11	8.0	50.0	20.4
12	8.0	50.0	20.4
<i>Steam pre-treated bone char</i>			
13	3.1	50.0	20.4
14	12.9	50.0	20.4
15	8.0	1.0	20.4
16	8.0	99.0	20.4
17	8.0	50.0	4.9
18	8.0	50.0	38.0
19	8.0	50.0	20.4
20	8.0	50.0	20.4

*Initial pH of the effluent was corrected to the desired pH. Without the correction, it was 9.0

Design of experiments and optimization

Experiments were carried out according to a central composite design (CCD), using three factors (pH, solid–liquid ratio and initial boron concentration) and two blocks (steam pre-treated and “in natura” bone chars), taking boron removal and variance as responses, according to Table 1. Samples were kept in a shaker, at 25.0 ± 0.1 °C, 180 ± 1 rpm, for 24 h.

Boron percentage removal was calculated according to Eq. 1. Initial (C₀) and final (C) concentrations were obtained from the Carmine method (4500B) in “Standard Methods for Examination of Water and Wastewater” (APHA 2017).

$$\% \text{Boron removal} = \frac{C_0 - C}{C_0} \quad (1)$$

Optimization for boron percentage removal was performed according to Generalized Reduced Gradient (GRG) method, using Excel® Solver tool. However, aiming at minimizing the variance and, at the same time, maximizing

boron uptake, a Pareto Frontier was constructed from Normal Boundary Intersection (NBI) algorithm (Paixão et al. 2019).

Kinetics studies

Three kinetics studies were performed at different temperatures (15.0 ± 0.1 °C, (25.0 ± 0.1) °C and (35.0 ± 0.1) °C. Boron adsorption onto bovine bone char was monitored over 48 h of experiments. From the design of experiments and optimization results (Sect. 3.2.1), the solid–liquid ratio selected for the kinetics studies was 59.95 g L⁻¹, with an initial effluent pH corrected to 7.72 and initial boron concentration of 18.63 mg L⁻¹. To determine the equilibrium time for each kinetics study, 13 experiments were carried out (05 min, 10 min, 15 min, 20 min, 25 min, 30 min, 1 h, 1 h 30 min, 3 h, 6 h, 12 h, 24 h and 48 h). Nonlinear pseudo-first-order, pseudo-second-order and Elovich models fit were evaluated.

Equilibrium study

Batch adsorption tests for equilibrium studies were performed by evaluating different solid–liquid ratios (2.5; 5.0; 10.0; 25.0; 50.0; 100.0; 200.0; and 400.0 g L⁻¹) at room temperature (25.0 ± 0.1 °C) for 6 h. Nonlinear Freundlich, Henry, Langmuir, Langmuir–Freundlich and Temkin isotherms models were fit to experimental data to obtain the parameters and describe the system.

Results and discussion

Adsorbent characterization

Particle size distribution for granular bovine bone char is shown in Fig. 1. It is observed that the parameters D50, D10 and D90 are equal to 0.70, 0.35 and 1.25 mm, respectively.

As the fraction retained between the 12.0–32.0 mesh (0.5–1.4 mm) sieves corresponded to 72.9% of the bone char sample, it was isolated and used in all experiments performed in order to standardize the adsorbent size for the adsorption process. In addition to greater availability, bovine bone char in the selected size can be used in both modes, batch and continuous systems.

Table 2 shows the surface area, the average diameter and the total pore volume for new non-treated and boron adsorbed bone chars.

New and boron adsorbed bone char presented surface area of 104 and 107 m² g⁻¹, respectively, thus, in accordance with previous studies. Nigri et al. (2016a, b) reported 139 m² g⁻¹,

and Ribeiro (2011), $119 \text{ m}^2 \cdot \text{g}^{-1}$, using bone char from the same supplier, to remove fluoride from aqueous solutions. Also, Tovar-Gómez et al. (2013) reported surface area from 104 to $129 \text{ m}^2 \cdot \text{g}^{-1}$, for bone chars from different suppliers, Meili et al (2018) and Mesquita et al (2017a, b), who used bovine bone char from the same supplier, for the adsorption of organic contaminants, reported surface areas of $94 \text{ m}^2 \cdot \text{g}^{-1}$ and $90 \text{ m}^2 \cdot \text{g}^{-1}$, respectively.

Mesoporous structure for both, new and boron adsorbed bone char, was also confirmed (average pore diameter of 7.25 and 7.55 nm and total pore volume of 0.1880 and $0.2010 \text{ cm}^3 \cdot \text{g}^{-1}$, respectively) by BJH pore distribution model. Thus, “adsorption proceeds via the consecutive formation of adsorbate layers which is completed by the phenomenon of capillary condensation” (White et al. 2009).

Figure 2 presents N_2 adsorption/desorption isotherms for both, new and boron adsorbed bone chars.

A hysteresis loop with non-parallel branches is observed, typical of pores whose size distribution is wide and shape is not well defined. Adsorption/desorption curve (Fig. 2) would be classified into Type V, according to Thommes et al. (2015), in their IUPAC Technical Report. According to the authors, for Type V isotherms shape, for low range of p/p_0 , relatively weak micro or mesoporous adsorbent-adsorbate interactions are present, what makes it, in this region, very similar to Type III isotherms; as p/p_0 increases, “molecular clustering is followed by pore filling”. The shape of hysteresis loop is very close to type H_3 , suggesting that the bone char could be constituted by non-rigid aggregates of plate-like particles or macropores of the pore network that are not completely filled (Thommes et al. 2015).

Indeed, X-ray diffraction (XRD) analysis showed a relatively amorphous material and few peaks could be distinguished in the analysis (Fig. 3), suggesting a proper crystalline structure of HAP could not be achieved either

Table 2 New and boron adsorbed bone chars surface areas and porosity

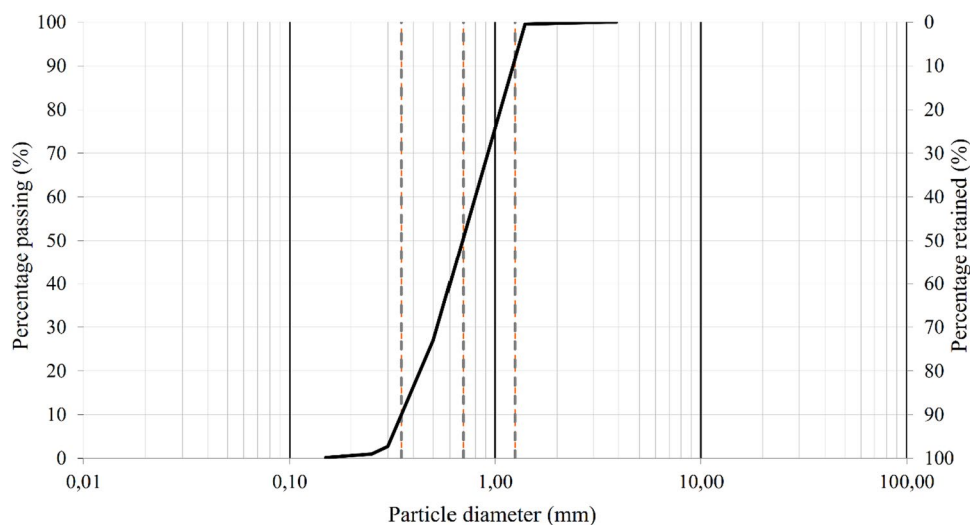
Bone char	Surface area ($\text{m}^2 \cdot \text{g}^{-1}$)	Mean diameter (Å)	Total pores volume ($\text{cm}^3 \cdot \text{g}^{-1}$)
New (non-treated)	104	72.5	0.19
Boron adsorbed (saturated)	107	75.5	0,20

during bone char production. Medellín-Castillo et al. (2016), while studying the influence of calcination temperature on crystalline phases, crystallite size, obtained similar results and contents of hydroxyapatite, monetite, and other calcium phosphates, present in their synthesized bone char.

As expected, XRD confirmed the presence of hydroxyapatite ($\text{Ca}_{10}(\text{PO}_4)_6(\text{OH})_2$) from the peaks corresponding to angles 25.9° , 31.7° , 40.0° , 46.7° and 49.5° (JCPDS 09-0432) and calcite (CaCO_3) in the peaks at angles of 23.0° , 29.4° , 36.0° , 48.5° and 64.7° (JCPDS 47-1743) (Flores-Cano et al. 2016; Nigri et al. 2016a). No changes among the samples of new and steam pre-treated bone char before and after adsorption with boron were noticed. As no new peaks were noticed before and after boron adsorption, it can be noticed that no formation of new minerals took place and the precipitation mechanism was not important for boron removal by the biochar.

FTIR analysis was used to detect changes in bone char structure after boron adsorption. Figure 4 shows the FTIR spectral bands of bovine bone char (black line) and after the boron adsorption process (red line). No significant changes were observed, except for the region of oxygen functional group bands (OH group at the range of $3303\text{--}3690 \text{ cm}^{-1}$) (Azevedo et al. 2017; Alkurdi et al. 2021). The bands at 470, 560, 600, 961 and 1023 cm^{-1} came from PO_4^{-3} ions, the last two being attributed to the stretching vibrations P-O and

Fig. 1 Particle size distribution for bovine bone char



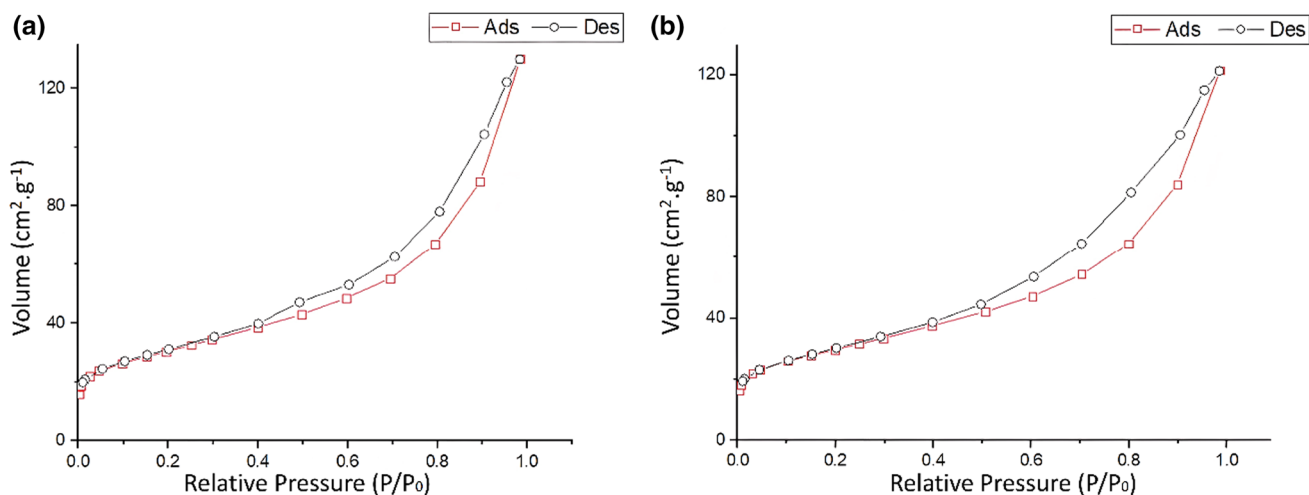


Fig. 2 N₂ adsorption/desorption isotherms for both, a new and b boron adsorbed bone chars

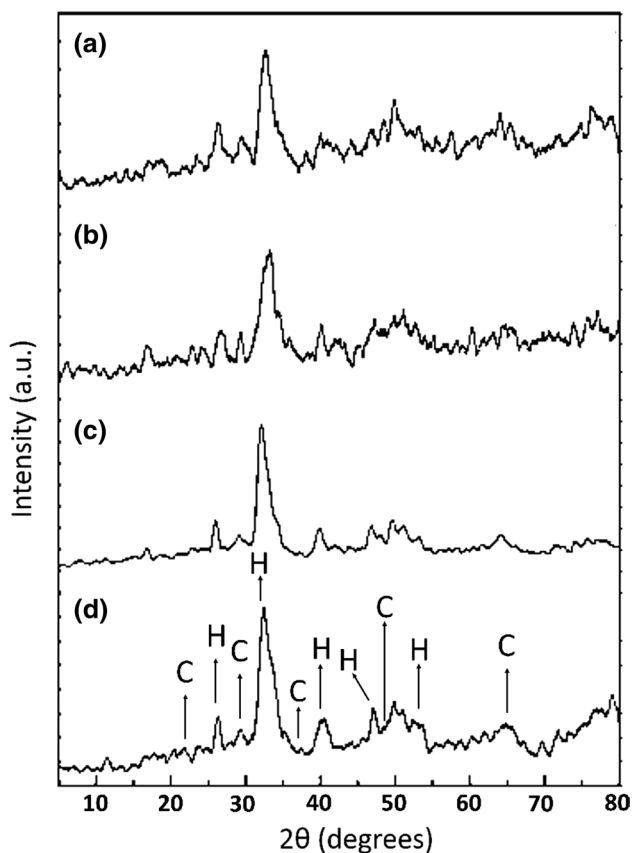


Fig. 3 Diffractograms for a steam pre-treated bone char and b non-pre-treated bone char, after the adsorption process to remove boron; c steam pre-treated new bone char and d non pre-treated new bone char. H=hydroxyapatite ($\text{Ca}_{10}(\text{PO}_4)_6(\text{OH})_2$) and C=calcite (CaCO_3)

the others corresponding to PO_4^{3-} bending vibrations (Patel et al. 2015; Jia et al. 2017). The C-O stretching vibrations at

1450, 1410 and 871 cm^{-1} has been assigned to CO_3^{2-} group (Patel et al. 2015).

Scanning electronic microscopy (SEM) for the same material, presented by Mesquita et al (2017a, b) in Fig. 5, shows high porosity and irregularities on the bone char surface. Rocha et al. (2011) identified chemical species on the particle surface of bone char by SEM and the authors observed high contents of calcium and phosphorous, as expected, being these the major elements, in accordance with the origin of the solid (cow bones, constituted of hydroxyapatite, which is the bearing phase of phosphorus).

The point of zero charge pH (pH_{PCZ}) of new bone char was 7.2 ± 0.1 , as shown in Fig. 6. Table 3 shows zeta potential and mean hydrodynamic diameter for new and boron adsorbed bone chars.

Mean hydrodynamic diameter is statistically the same before and after boron adsorption, but zeta potential shows that boron adsorption leads to a decrease (in module) of the negative potential. In other words, the results suggest the uptake of some positively charged compound in the conditions analyzed.

Lin et al (2021) reports “the major species of boron in aqueous solution is boric acid ($\text{B}(\text{OH})_3$), a weak acid with pKa value of 9.2, and its conjugate base ($\text{B}(\text{OH})_4^-$) that predominates in alkaline condition”. The optimized pH of boron adsorbed bone char was 7.8 and analyses were, then, carried out within these conditions. Zeta potential and pH_{PCZ} confirmed negatively charged adsorbent; thus electrostatic interaction would not be a potential mechanism for boron adsorption. Indeed, optimization analyses (addressed appropriately in the next sections) showed that the more alkaline the medium became, the more boron removal diminished, due to repulsion between ($\text{B}(\text{OH})_4^-$) and the negatively charged solid.



Fig. 4 FTIR analyses for a new and b boron saturated bovine bone char

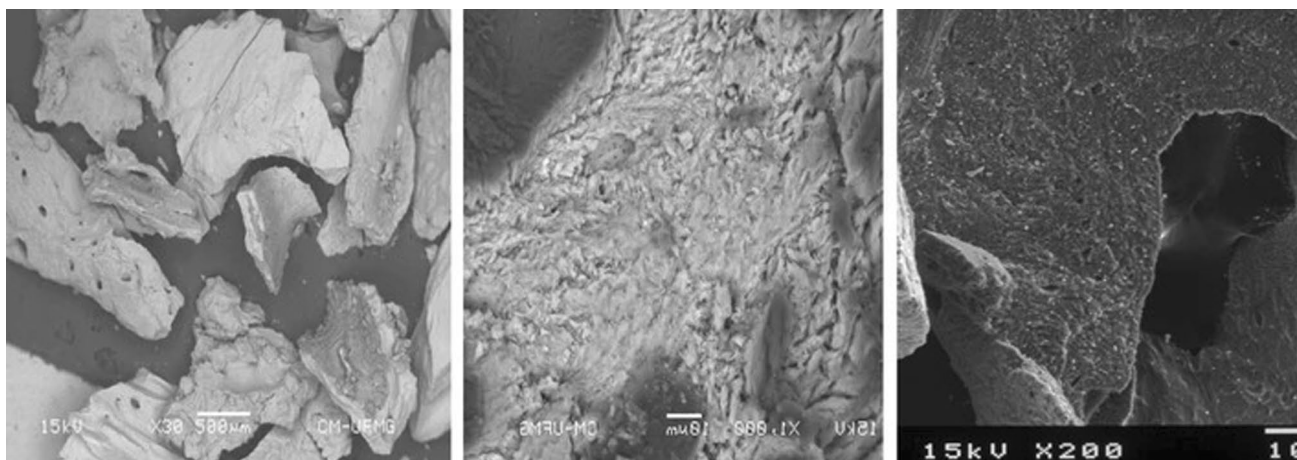
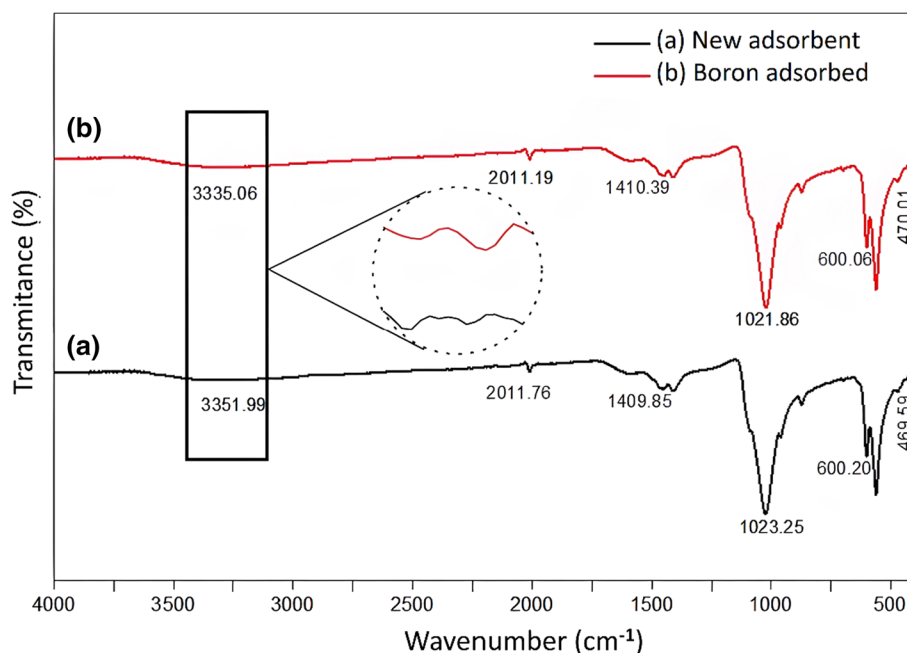
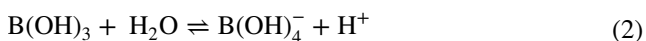


Fig. 5 Scanning electronic microscopy (SEM) images for bone char (Mesquita et al. 2017a, b)

Besides HAP, calcite (CaCO_3) is also present in bone char, as previously observed. Thus, Ca^{2+} is available in the solution and at $\text{pH} > \text{pH}_{\text{PCZ}}$, a positively charged boron compound will emerge, as expressed by Eqs. 2 and 3:



According to Demetriou et al. (2013), the hydroxyl groups on the hydrous surface of metal oxides and hydroxides are capable of forming borate esters like chelating functional groups, as boric acid is known to have a great

affinity with polyols through chelating mechanism. Also, as stated by Lin et al (2021), the neutral surface group, $\equiv\text{MeOH}$, will be protonated as $\equiv\text{MeOH}_2^+$ at low pH and deprotonated as $\equiv\text{MeO}^-$ at high pH, and boron removal by the metal-based adsorbents is rather pH-sensitive. Indeed, Medellín-Castillo et al. (2016) also observed that the oxygenated groups attached to the carbon may also be deprotonated and protonated to form acidic and basic sites, and this seems to be the case, as HAP seems quite stable and no changes were observed in the corresponding HAP bands, even when boron is present, similar to what was reported by Yang-Zhou et al. (2021), indicating that “the borate ions were not removed by replacing the phosphate radical of precipitates in HAP” (Yang-Zhou et al, 2021).



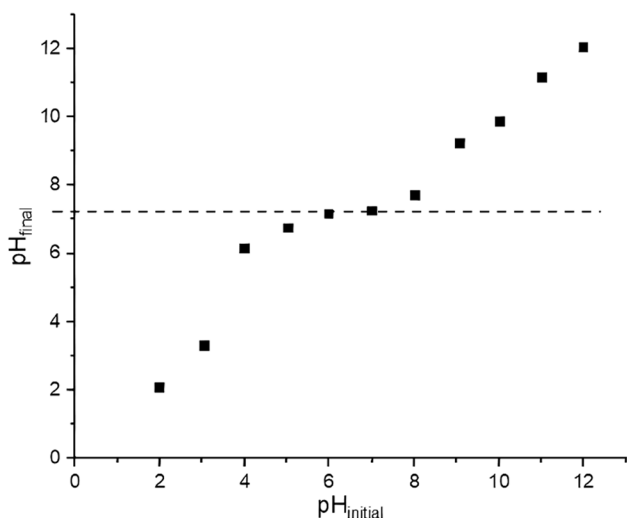


Fig. 6 Curve of pH at point of zero charge (PZC)

Thus, similar to what has happened to Liu et al. (2021), B was removed as negatively adsorbed $[\text{CaB}(\text{OH})_4]^+$, suggesting occlusion co-precipitation mechanism (Fig. 7).

Another important discussion and confirmation is about the limitation of boron uptake under the conditions analysed, taking into account the mechanism: $\text{B}(\text{OH})_4^-$ starts to appear at $\text{pH} = 6.0$ and at $\text{pH} = 7.8$ (condition investigated), very low concentration of $\text{B}(\text{OH})_4^-$ is present, leading to a low $[\text{CaB}(\text{OH})_4]^+$ availability. Furthermore, as bovine bone char has about 9 to 11% calcite and carbon and 75% hydroxyapatite, which is relatively stable and does not easily release large amounts of Ca ions, the formation of $[\text{CaB}(\text{OH})_4]^+$ and its consequent adsorption onto the bone char surface is low (Nigri et al. 2016b; Yang-Zhou et al. 2021), what explains the low adsorption capacity for boron uptake.

Fig. 7 Schematic diagram for boron removal mechanism onto bovine bone char

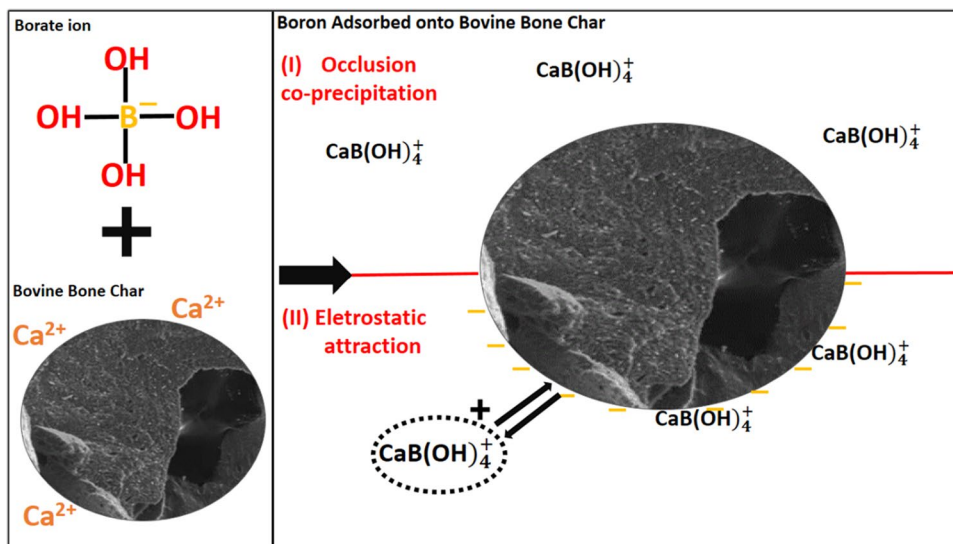


Table 3 New and boron adsorbed zeta potential and mean hydrodynamic diameter

	New bone char	Boron adsorbed bone char
Zeta potential (mV)	-22.9 ± 3.3	-17.8 ± 0.4
Mean hydrodynamic diameter (nm)	184.7 ± 6.5	182.4 ± 3.7

Adsorption studies

Design of experiments and optimization

From the complete factorial design using 3 factors and 4 central points, it was possible to confirm the presence of curvature (p value = 0.027), which showed that the chosen levels were adequate for building a response surface and obtaining a quadratic model for the quantification of boron removal. For the construction of the CCD, experiments related to axial points, two central points and the block corresponding to steam-treated bone char were added, results presented in Table 4.

Analysis of variance (ANOVA) was performed and the results are shown in Table 5.

The predicted model presented satisfactory fit (from p value analysis and $R^2_{\text{Adjust}} = 95.3\%$) to represent boron percentage removal by bone char under the adopted conditions ($T = 25.0 \pm 0.1$ °C; rotation = 180 ± 1 rpm; time = 24 h).

The main factors evaluated were significant for boron removal, except for the interactions between two factors and the square interaction of initial boron concentration in the effluent. The difference between the blocks concerning pre-treatment taking boron percentage removal as response was not significant (p value = 0.726). Thus, the

Table 4 CCD results for boron removal by bovine bone char ($T=25.0\pm 0.1\text{ }^\circ\text{C}$; rotation = $180\pm 1\text{ rpm}$; time = 24 h)

Blocks*	pH	Solid/liquid ratio (g L^{-1})	Initial concentration of boron (mg L^{-1})	Boron removal (%)
1	5.00	20.00	15.00	22.22
1	11.00	20.00	15.00	11.11
1	5.00	80.00	15.00	55.98
1	11.00	80.00	15.00	46.30
1	5.00	20.00	40.00	10.17
1	11.00	20.00	40.00	7.45
1	5.00	80.00	40.00	37.29
1	11.00	80.00	40.00	32.20
1	8.00	50.00	27.50	33.33
1	8.00	50.00	27.50	39.22
1	8.00	50.00	27.50	33.33
1	8.00	50.00	27.50	39.22
2	3.10	50.00	27.50	31.37
2	12.90	50.00	27.50	9.80
2	8.00	1.01	27.50	1.96
2	8.00	98.99	27.50	56.86
2	8.00	50.00	7.09	48.98
2	8.00	50.00	47.91	26.32
2	8.00	50.00	27.50	33.33
2	8.00	50.00	27.50	41.18

*Block 1 represents experiments using new bone char and block 2, experiments using steam pre-treated bone char

steam pre-treatment did not contribute to an improvement in adsorption, which corroborates the characterization study described previously.

Figure 8 shows Pareto plot for standardized effects and the residue analysis for boron percentage removal by bone char. Figure 8a indicates the importance of the solid–liquid ratio in the process of boron uptake by bovine bone char, as this factor and its quadratic interaction exceeded the critical F value in the standardized effect. Besides, Fig. 8b shows that the residues are distributed in a normal way, which confirms an accurate execution of experiments (Naves et al. 2016; Paixão et al. 2019).

To assess how boron removal was influenced by the levels of each factor, the main effects analysis was performed, as shown in Fig. 9, and is explained as follows.

Effect of initial pH of the effluent

Initial pH of the effluent effect was studied for the pH range from 3 to 13 (Fig. 9a). It is known that pH of the solution affects the distribution of boron species, such as $\text{B}(\text{OH})_3$ and $\text{B}(\text{OH})_4^-$. Boron adsorption depends on which boron species are dominant in the solution (Bursalı et al. 2011). In this work, the dependence of initial pH of the effluent for boron uptake by bone char showed that, with the increase in pH, boron removal tended to increase to a maximum (almost 40%) at pH between 7 and 8. In fact, in acidic solutions, where boric acid ($\text{B}(\text{OH})_3$) predominates, the removal of boron is inferior compared

Table 5 Analysis of variance (ANOVA) of CRCD for the removal of boron by bovine bone char ($T=25.0\pm 0.1\text{ }^\circ\text{C}$; rotation = $180\pm 1\text{ rpm}$; time = 24 h)

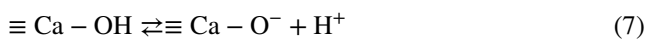
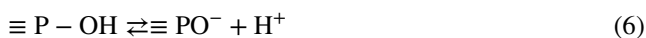
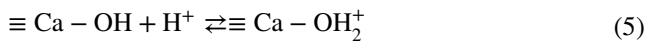
Source	DF*	SS*	MS*	Value F*	Value P*
Model	10	4812.86	481.29	39.88	0.000
Block	1	1.58	1.58	0.13	0.726
Linear	3	4176.16	1392.05	115.34	0.000
pH	1	305.48	305.48	25.31	0.001
Solid/liquid ratio (g.L^{-1})	1	3322.31	3322.31	275.27	0.000
Initial concentration (mg L^{-1})	1	548.38	548.38	45.44	0.000
Square	3	577.48	192.49	15.95	0.001
pH * pH	1	492.92	492.92	40.84	0.000
Solid/liquid ratio * solid/liquid ratio	1	103.58	103.58	8.58	0.017
Initial concentration * Initial Concentration	1	1.09	1.09	0.09	0.77
Interaction with 2 factors	3	57.63	19.21	1.59	0.259
pH* solid/liquid ratio	1	0.11	0.11	0.01	0.926
Ph* initial concentration	1	21.09	21.09	1.75	0.219
Solid/liquid ratio * initial concentration	1	36.43	36.43	3.02	0.116
Error	9	108.62	12.07		
Lack of adjustment	5	43.26	8.65	0.53	0.749
Pure error	4	65.36	16.34		
Total	19	4921.48			
Model	R ² :	97.79%	R ² _{Adjust} :	95.34%	

*DF degree of freedom, SS sum of squares, MS mean square and F statistics F value

to neutral solutions due to the lack of electrostatic attraction (Oladipo and Gazi 2016). According to Kabay et al. (2015), the removal of boron at acid pH is low, due to the lack of charge of unionized boric acid (B(OH)₃), while in the ionic form of borate (B(OH)₄⁻), in addition to being more hydrated.

Moreover, the surface charge of the adsorbent is also important to explain the adsorption of ions onto bone char and occurs due to the interactions between the ions present in the solution and the functional groups on bone char surface (Sasaki et al. 2016). According to Medellin-Castillo et al. (2016), phosphate groups and hydroxyls on the surface of bovine bone char are protonated, providing a positive charge to the adsorbent surface (Equations 4 and 5). On the other hand, the negative charge on the

surface of the bone char is provided by the deprotonation of the phosphate and hydroxyl groups (Equations 6 and 7):



where ≡ represents the bone char surface. Protonation reactions occur at pH < pH_{PZC}, and deprotonation at pH > pH_{PZC},

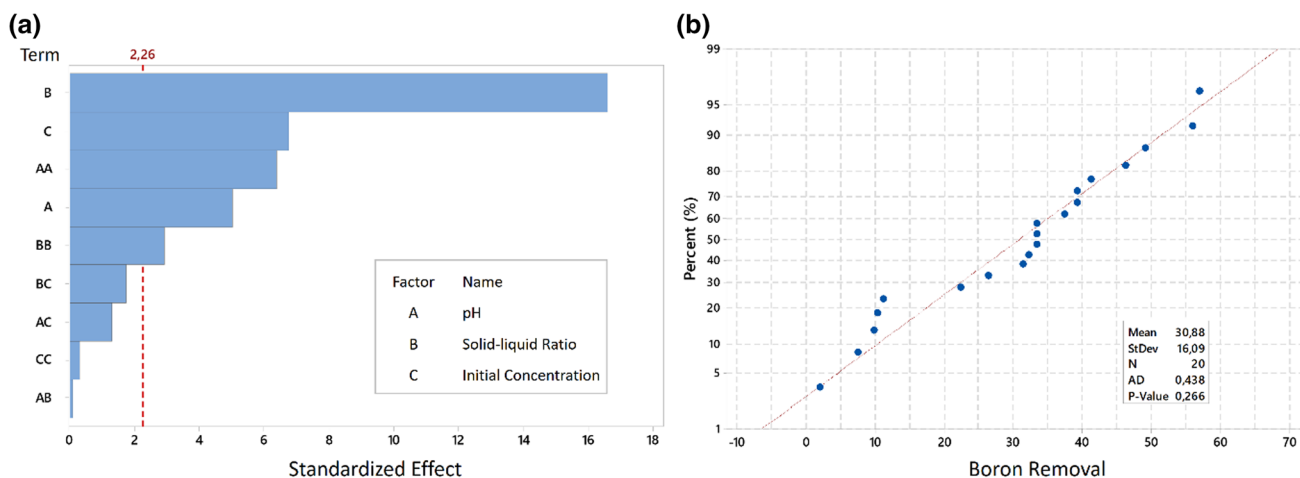
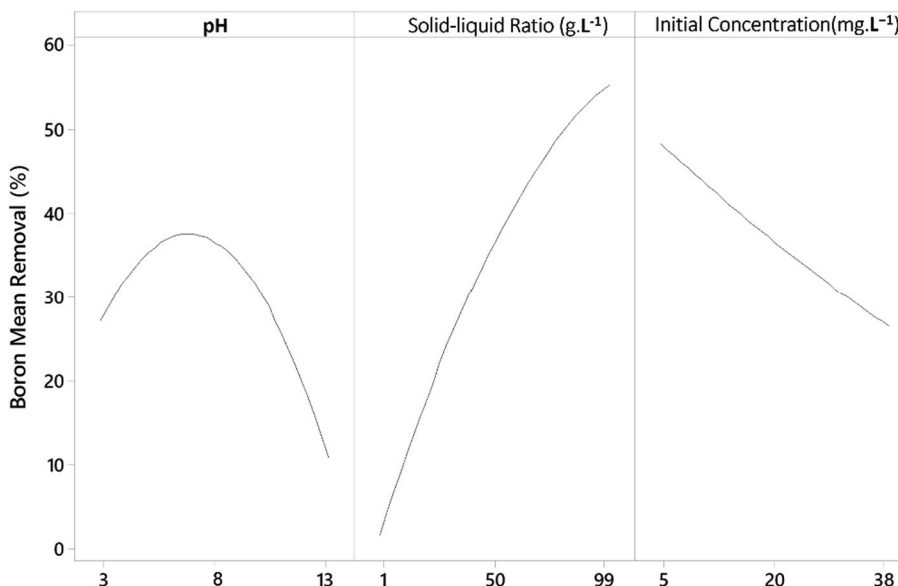


Fig. 8 Pareto chart for standardized effects (a) and residue analysis (b) for boron removal by adsorption on bovine bone char ($T=25.0 \pm 0.1$ °C; rotation = 180 ± 1 rpm; time = 24 h)

Fig. 9 Main effects of the design of experiments (CCD) for boron percentage removal by bovine bone char ($T=25.0 \pm 0.1$ °C; rotation = 180 ± 1 rpm; time = 24 h)



where pH_{PZC} (point of zero charge) is the pH at which the surface charge is zero (Nigri et al. 2016b). Therefore, the pH directly affected the adsorption of boron. In pH of the solution around pH_{PZC} (7.2 ± 0.1), as previously seen and now emphasized, the boron removal mechanism onto bovine bone char involved occlusion co-precipitation of $\text{CaB}(\text{OH})_4^+$, followed by electrostatic interactions between this compound and the negative charged surface of the adsorbent. However, as previously discussed, due to the low availability of Ca^{2+} for the formation of $[\text{CaB}(\text{OH})_4]^+$ and also due to the rise of borate ion concentration at pH above 8 and its predominance at those superior to 9.2 (pKa), the electrostatic repulsion between this ion and the negative surface of bone char disfavored boron uptake.

Effect of solid–liquid ratio

Solid–liquid ratios used in this study were between 1.01 and 98.99 g L^{-1} (Fig. 9b). Boron removal increased significantly (55%) with the increase in the solid–liquid ratio, achieving 57% removal for the highest solid–liquid ratio tested and 2% for the lowest solid–liquid ratio. This fact is direct related to the increased availability of active sites to remove the contaminant.

Effect of the initial boron concentration in the effluent

The increase of the initial boron concentration in the effluent, from 5 to 38 mg L^{-1} , led to a reduction in the percentage of its removal from 49 to 26% (Fig. 9c). In contrast, as shown in Fig. 10, the boron adsorption capacity increased with increasing initial concentration.

Demey et al. (2014) in the study of adsorption of boron by chitosan/ $\text{Ni}(\text{OH})_2$ -based adsorbent stated that increasing the boron concentration increased the concentration gradient between the solution and the surface of the adsorbent. As a consequence, the driving force increased as well as the adsorption rate. Therefore, to analyze the effect of the initial concentration, it is necessary to evaluate together with the amount of adsorbent used in the experiments, as the removal percentage does not show the amount of adsorption sites occupied by the adsorbate (Alkurdi et al. 2019).

Optimization

From the GRG algorithm, the conditions to maximize the boron percentage removal by adsorption onto bovine bone char were: initial effluent pH of 7.31, solid–liquid ratio of 80.22 g L^{-1} and initial boron concentration of 12.91 mg L^{-1} .

However, as the response surfaces are concave, the need to maximize boron removal was found in a region very close

to the boundary conditions ($X^T X < \alpha$), which represents the hyperplane established by the response surface. Thus, optimization, in terms of the convexity of the objective function of the response surface, can lead to high values of boron removal, however with large variances, since points more distant from the central points correspond to greater associated variances (Naves et al. 2016). In this context, using the NBI method and iteratively varying the weights from 0 to 1, the equispaced Pareto frontier (Fig. 11) was obtained, relating the process variance to boron removal.

The selected conditions to carry out the following experiments, highlighted in Fig. 11 (pH 7.72, solid–liquid ratio of 59.95 g L^{-1} and initial boron concentration of 18.63 mg L^{-1}) was chosen due to three main practical reasons, from the process point of view. The pH was closer to the value that does not demand correction (9.0), representing savings in chemicals. The solid–liquid ratio was about 25% lower than necessary for the condition of the highest boron removal (57.7%), representing savings in the amount of adsorbent to be purchased. Finally, this condition showed one of the smallest variances, being possible to reach 43.3% of boron removal with a variance of $2.2\%^2$, while for the highest boron removal the variance was around three times higher ($6.7\%^2$). Reducing the variance associated to boron removal process is extremely important because, in addition to making the process more stable, it may bring about a reduction in variability in subsequent scale up, which would facilitate application without using pilot scales.

In fact, when analyzing the control chart of individual values to monitor the stability of the process, there was an oscillation in the data related to the boron removal experiments for the response surface (Fig. 12a). In this case, the variability was high and the control limits are unreliable, within a range of 82.8%. However, when using the points determined from the NBI (Fig. 12b), it is noticed that the control limits calculated with the variation within the group

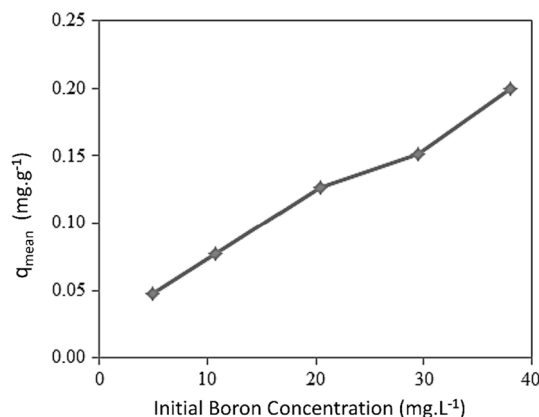


Fig. 10 Boron adsorption capacity for different initial concentration of adsorbate ($T = 25.0 \pm 0.1 \text{ }^\circ\text{C}$; rotation = $180 \pm 1 \text{ rpm}$; time = 24 h)



reduced to an amplitude of 5.6%. It is also possible to verify that the central region of the Pareto frontier (dots) is within the control limits. Thus, the Pareto frontier adjusts the variance values associated to boron removal.

Figure 13 shows the removal of boron as a function of each of the factors studied under conditions optimized by the NBI and confirms the previous discussion on the main effects.

Finally, to verify the consistency and efficiency of conditions optimized by the NBI, it was applied the One-Sample-T test. After carrying out 5 validation experiments, an average of 43% for boron removal and 3% for standard deviation were obtained, which demonstrated the effectiveness of the model. This was also proven by the p value of 0.656, obtained from the hypothesis test.

Adsorption isotherms

Figure 14 shows boron percentage removal and the adsorptive capacity as a function of the solid–liquid ratio, using bovine bone char as an adsorbent. It was possible to observe that boron removal was favored with the increase of the solid–liquid ratio, reaching $81 \pm 2\%$ for the highest solid–liquid ratio tested (400 g L^{-1}), which confirms the results discussed previously.

Freundlich, Langmuir, Tenkim, Henry and Langmuir–Freundlich isotherms were fit to experimental data and the parameters are presented in Table 6 and the nonlinear fits to the experimental data are shown in Fig. 15.

Although the tested models presented high determination coefficients ($R^2 > 0.94$), indicating good fit, the Freundlich model best described the system, under the evaluated conditions, considering the values of the parameters ($R^2 = 0.9970$). Sasaki et al (2016) also had borate sorption data in precipitated hydroxyapatite adjusted to the Freundlich model. The Freundlich equation suggests a heterogeneous system and a reversible adsorption process, which is not necessarily restricted to the formation of monolayers (Delazare et al. 2014).

It was also noticed that the value of n , which indicates the intensity of adsorption, was close to unit (0.9345). The n value is a measure of linearity, so, when n is equal to the unit, the process involves linear adsorption, in which the sites exhibit equivalent sorption energies and there is no interaction between the adsorbed species. For values of inferior to the unit, the interaction between the adsorbate and the adsorbent is weak (Delazare et al. 2014).

Although the maximum boron adsorption capacity in bovine bone char found experimentally in this study was low, 0.24 mg g^{-1} , it is still superior to other adsorbents found in the literature, such as vermiculite (0.16 mg g^{-1}) (Kehal et al. 2010), sepiolite (0.16 mg g^{-1}), illite (0.11 mg g^{-1}) (Karahana et al. 2006).

Kinetics study

As changes in temperature influence the adsorbent capacity at equilibrium for a given adsorbate, boron adsorption onto bovine bone char was monitored over 48 h of experiments at

Fig. 11 Pareto frontier obtained by NBI optimization. Conditions of the highlighted point of pH 7.72, solid–liquid ratio of 59.95 g L^{-1} and initial boron concentration of 18.63 mg L^{-1} ($T = 25.0 \pm 0.1 \text{ }^\circ\text{C}$; rotation = $180 \pm 1 \text{ rpm}$; time = 24 h)

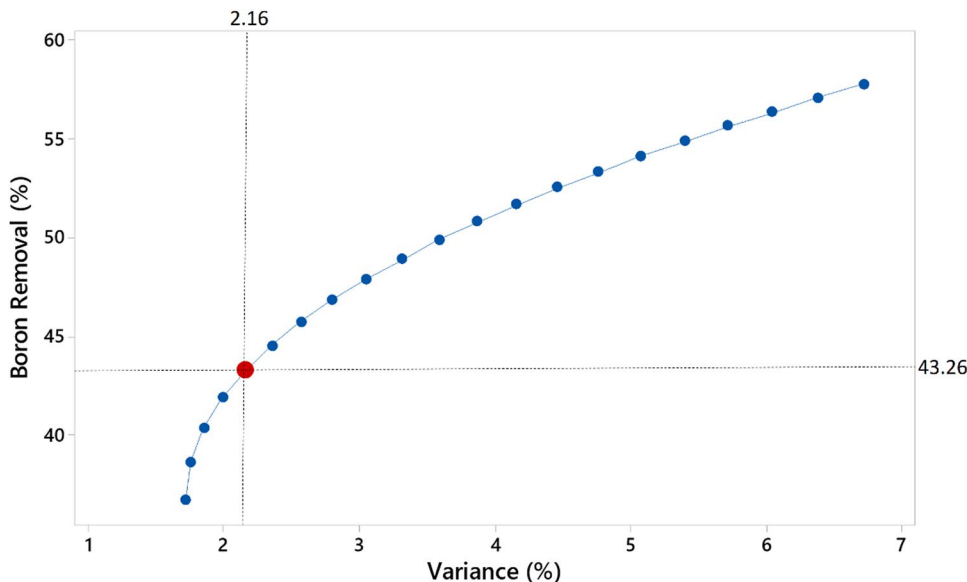


Fig.12 Control chart for individual values in relation to boron removal results obtained from: CCD experiments (a) and NBI optimization (b)

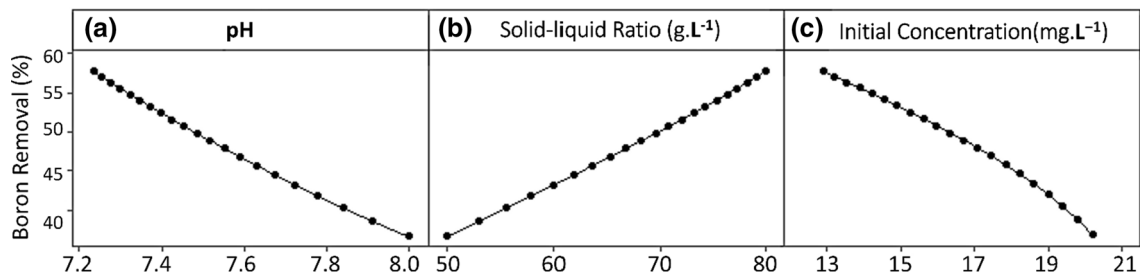
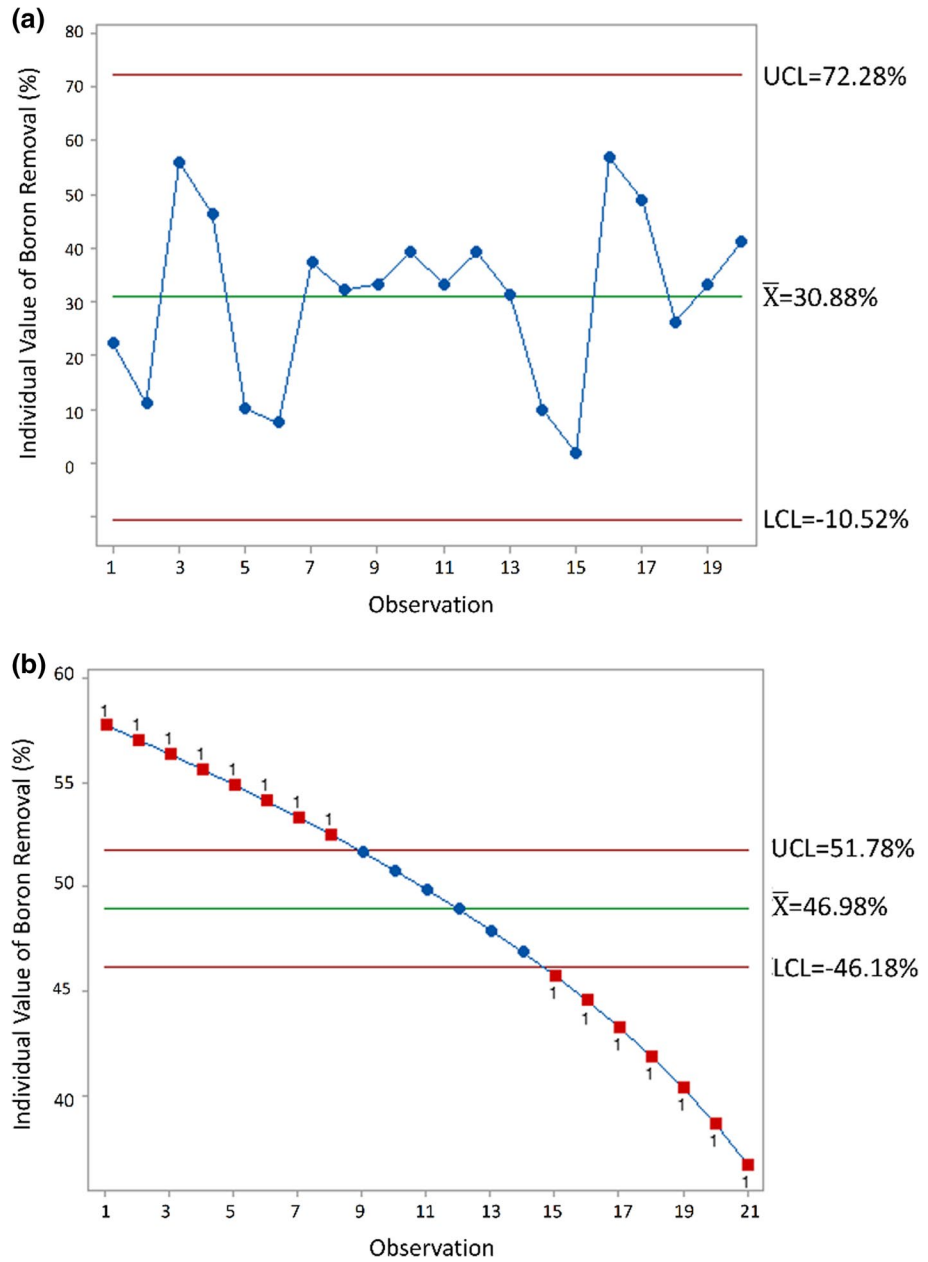


Fig. 13 Boron removal as a function of each factor: pH (a), solid–liquid ratio (b), initial boron concentration (c) under conditions optimized by the NBI

Fig. 14 Boron removal (a) and adsorptive capacities (b) for different solid–liquid ratios (temperature = 25.0 ± 0.1 °C, rotation = 180 ± 1 rpm, pH = 7.8; C₀ = 18.63 mg L⁻¹)

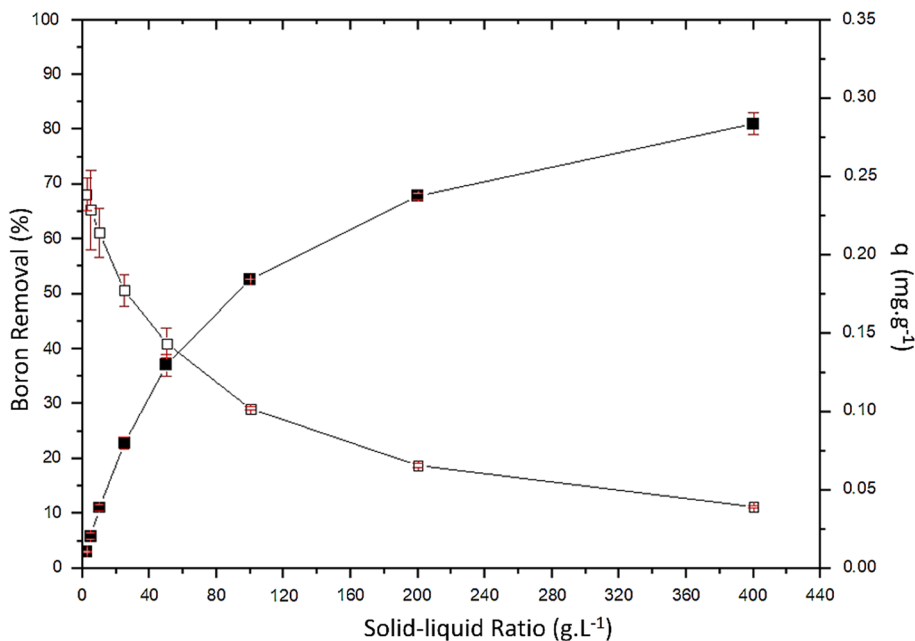


Table 6 Isotherms parameters for boron removal by bone char (temperature = 25.0 ± 0.1 °C, pH = 7.7 ± 0.1, C₀ = 18.63 mg L⁻¹, 180 ± 1 rpm)

Freundlich: $q_e = K_f \cdot C_e^{\frac{1}{n}}$			
K_f	n	Statistical parameter	
($\text{mg g}^{-1}(\text{L mg}^{-1})^{1/n}$)		(R^2)	
0.0096 ± 0.0004	0.9345 ± 0.0186	0.9970	
Langmuir: $q_e = \frac{q_{\max} \cdot K_L \cdot C_e}{1 + K_L \cdot C_e}$			
q_{\max}	K_L	Statistical parameter	
(mg g^{-1})	(L mg^{-1})	(R^2)	
1.071 ± 0.0000	0.0111 ± 0.0003	0.9762	
Temkin: $q_e = q_t \ln(1 + K_T \cdot C_e)$			
q_t	K_T	Statistical parameter	
($\text{mg} \cdot \text{g}^{-1}$)	(L mg^{-1})	(R^2)	
0.3244 ± 0.0115	0.0401 ± 0.0017	0.9771	
Henry: $q_e = K_{HE} \cdot C_e$			
K_{HE}	Statistical parameter		
(L g^{-1})	(R^2)		
0.0110 ± 0.0002	0.9928		
Langmuir–Freundlich: $q_e = \frac{q_{\max} \cdot K_{lf} \cdot C_e^{n_{lf}}}{1 + K_{lf} \cdot C_e^{n_{lf}}}$			
q_{\max}	K_{lf}	n_{lf}	Statistical parameter
(mg g^{-1})	$((\text{mg g}^{-1})^{n_{lf}})$ ($\text{L mg}^{-1})^{n_{lf}}$)		(R^2)
1.071 ± 0.0000	0.0083 ± 0.0006	1.1508 ± 0.0339	0.9935

three different temperatures (15.0 ± 0.1 °C, 25.0 ± 0.1 °C and 35.0 ± 0.1 °C) and the results are shown in Fig. 16.

Kinetics data shows marked removal of boron, in the first hour of experiment, when average 25% of boron removal was achieved. At temperatures of 15.0 ± 0.1 °C and 25.0 ± 0.1 °C, approximately 70% of the adsorption capacity at equilibrium was reached in the first 30 min. However, for all three temperatures, the adsorption speed decreased after the first hour, due to the initial availability of a large number of active sites on the surface, which are gradually filled until equilibrium is reached (Alkurdi et al. 2019). At temperatures of 15.0 ± 0.1 °C and 25.0 ± 0.1 °C, it took 6 h to reach equilibrium, while for the temperature of 35.0 ± 0.1 °C, the equilibrium was reached only after 12 h.

At 15.0 ± 0.1 °C, the adsorptive capacity, q_e , was 0.106 ± 0.005 mg g⁻¹, and boron removal, 33 ± 1%. At 25.0 ± 0.1 °C, q_e was 0.121 ± 0.003 mg g⁻¹ and boron removal, 38 ± 1%. For a temperature of 35.0 ± 0.1 °C, an increase in adsorptive capacity and percentage removal was observed (0.134 ± 0.009 mg g⁻¹ and 44.5 ± 0.5%, respectively). Increasing temperature leads to enhancing diffusion rate of adsorbed molecules through external and internal pore layers, due to decrease in viscosity of the solution (Mesquita et al. 2017a).

Pseudo-first, pseudo-second and Elovich models were evaluated and parameters and determination coefficients are shown in Table 7.

The adsorption kinetics for boron uptake by bone char was well described by the pseudo-second order model, as well as for almost all sorbents of natural materials (Guan

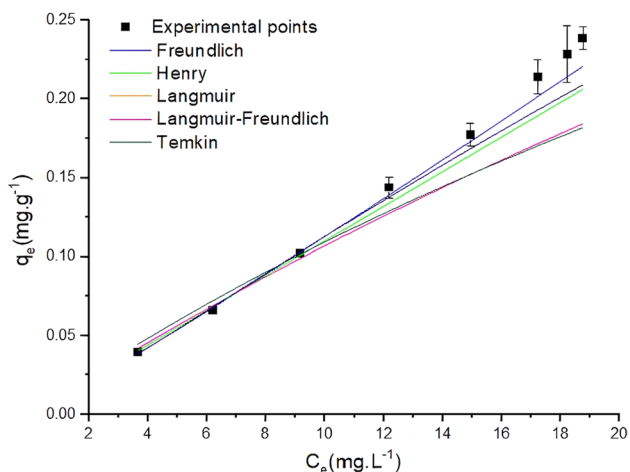


Fig. 15 Adsorption isotherms for boron removal from bone char (temperature = 25.0 ± 0.1 °C, rotation = 180 ± 1 rpm, pH = 7.8; $C_0 = 18.63$ mg L⁻¹)

et al. 2016). The pseudo-second-order model assumes that the difference between the concentration in the solid phase at any time *t* and in equilibrium is the driving force of the adsorption and that the overall rate of adsorption is the square of the driving force (Haghi et al. 2017). According to Simonin (2016), a diffusion-controlled process is better

described by the pseudo-second-order model, compared to the pseudo-first-order model.

Conclusion

Bovine bone char, particle size of 12.0–32.0 mesh (0.5–1.4 mm), was able to remove, partially, by adsorption, boron present in a synthetic effluent. This adsorbent presented surface area of 104 m² g⁻¹, with mesoporous structure (diameter of 72.5 Å and total pore volume of 0.19 cm³ g⁻¹), being formed predominantly by hydroxyapatite (Ca₁₀(PO₄)₆(OH)₂), and calcite (CaCO₃).

Initial effluent pH, initial boron concentration and solid–liquid ratio were significant variables in the process. It was possible to remove 81% of boron, for the highest tested solid–liquid ratio (400 g L⁻¹). However, aiming at maximizing boron removal and, at the same time, minimizing process variance, the conditions of initial effluent pH of 7.72, solid–liquid ratio of 59.95 g L⁻¹ and initial boron concentration of 18.63 mg L⁻¹ were selected as the optimal conditions, leading to 43% of boron removal, with a variance of only 2%.

Equilibrium was well represented by Freundlich isotherm, showing proximity to a linear isotherm, indicating that the

Fig. 16 a Adsorptive capacities and b boron removal as a function of time, at temperatures of 15.0 ± 0.1 °C, 25.0 ± 0.1 °C and 35.0 ± 0.1 °C for 48 h (ratio = 59.95 g L⁻¹, pH = 7.72 ± 0.1 , 180 ± 1 rpm)

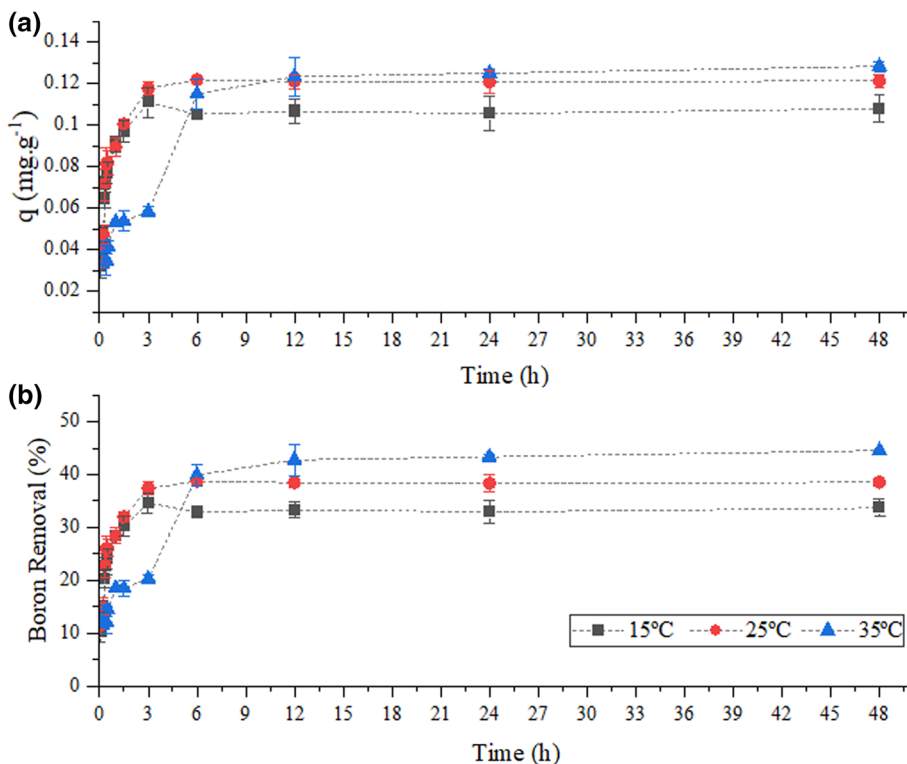


Table 7 Kinetics parameters for boron adsorption onto bovine bone char (solid–liquid ratio = 59.95 g L⁻¹, pH = 7.7 ± 0.1, C₀ = 18.63 mg L⁻¹, 180 ± 1 rpm)

T (°C)	Pseudo-second-order parameters		
	k_2 (g mg ⁻¹ min ⁻¹)	q_e (mg g ⁻¹)	R^2
15.0 ± 0.1	36.8037	0.1110	0.9737
25.0 ± 0.1	28.6159	0.1238	0.9656
35.0 ± 0.1	6.2529	0.1279	0.8294

T (°C)	Pseudo-second-order parameters		
	k (min ⁻¹)	q_e (mg g ⁻¹)	R^2
15.0 ± 0.1	2.7365	0.1051	0.9651
25.0 ± 0.1	2.4990	0.1163	0.9224
35.0 ± 0.1	0.4989	0.1207	0.7534

T (°C)	Elovich parameters		
	α (mg g ⁻¹ min ⁻¹)	β (g mg ⁻¹)	R^2
15.0 ± 0.1	6.3536	80.7824	0.7746
25.0 ± 0.1	4.2493	67.7517	0.8299
35.0 ± 0.1	0.5002	53.9227	0.8757

adsorption process can be reversible. The pseudo-second-order kinetics model showed the best fit.

Acknowledgements CAPES (Coordenação de Aperfeiçoamento de Pessoal de Nível Superior) and Federal University of São João del-Rei are gratefully acknowledged. The authors thank UFMG Mining Engineering Characterization Laboratory for FTIR analyses and UFOP CiPharma multiuser Laboratory for measures in NanoZeta Sizer.

author contributions All authors contributed to the study, read it and approved the final manuscript.

Funding This work was partially supported by CAPES (Coordenação de Aperfeiçoamento de Pessoal de Nível Superior) and Federal University of São João del-Rei.

Data availability The datasets generated during and/or analysed during the current study are available from the corresponding author on reasonable request.

Declarations

Conflict of interest The authors have no relevant financial or non-financial interests to disclose.

References

ABNT (2001) ABNT NBR NM 27:2001-Agregados-Redução da amostra de campo para ensaios de laboratório. Rio de Janeiro

Alkurdi SSA, Al-juboori RA, Bundschuh J, Hamawand I (2019) Bone char as a green sorbent for removing health threatening fluoride

from drinking water. *Environ Int* 127:704–719. <https://doi.org/10.1016/j.envint.2019.03.065>

- Alkurdi SSA, Al-juboori RA, Bundschuh J et al (2021) Inorganic arsenic species removal from water using bone char: a detailed study on adsorption kinetic and isotherm models using error functions analysis. *J Hazard Mater* 405:124112. <https://doi.org/10.1016/j.jhazmat.2020.124112>
- APHA (2017) Standard methods for the examination of water and waste-water (12th ed.), 23 edn. American Public Health Association, American Water Works Association, Water Environment Federation, Washington
- Asgari G, Dayari A, Ghasemi M et al (2019) Efficient fluoride removal by preparation, characterization of pyrolysis bone: Mixed level design experiment and Taguchi L 8 orthogonal array optimization. *J Mol Liq* 275:251–264. <https://doi.org/10.1016/j.molliq.2018.10.137>
- Ban SH, Im SJ, Cho J, Jang A (2019) Comparative performance of FO-RO hybrid and two-pass SWRO desalination processes: boron removal. *Desalination* 471:114114. <https://doi.org/10.1016/j.desal.2019.114114>
- Brdar-Jokanović M (2020) Boron toxicity and deficiency in agricultural plants. *Int J Mol Sci*. <https://doi.org/10.3390/ijms21041424>
- Bursalı EA, Seki Y, Seyhan S et al (2011) Synthesis of chitosan beads as boron sorbents. *J Appl Polym Sci* 122:657–665. <https://doi.org/10.1002/app.33331>
- Chen D, Zhao X, Li F, Zhang X (2016) Influence of surfactant fouling on rejection of trace nuclides and boron by reverse osmosis. *Desalination* 377:47–53. <https://doi.org/10.1016/j.desal.2015.09.002>
- Chen Z, Taylor AA, Astor SR et al (2017) Removal of boron from wastewater: evaluation of seven poplar clones for B accumulation and tolerance. *Chemosphere* 167:146–154. <https://doi.org/10.1016/j.chemosphere.2016.09.137>
- Chen M, Dollar O, Shafer-Peltier K et al (2020) Boron removal by electrocoagulation: removal mechanism, adsorption models and factors influencing removal. *Water Res* 170:115362. <https://doi.org/10.1016/j.watres.2019.115362>
- Cheng S, Zhang L, Xia H et al (2017) Adsorption behavior of methylene blue onto waste-derived adsorbent and exhaust gases recycling. *RSC Adv* 7:27331–27341. <https://doi.org/10.1039/c7ra01482a>
- Chorghé D, Sari MA, Chellam S (2017) Boron removal from hydraulic fracturing wastewater by aluminum and iron coagulation: mechanisms and limitations. *Water Res* 126:481–487. <https://doi.org/10.1016/j.watres.2017.09.057>
- Cruz MAP, Guimarães LCM, da Costa Júnior EF et al (2019) Adsorption of crystal violet from aqueous solution in continuous flow system using bone char. *Chem Eng Commun*. <https://doi.org/10.1080/00986445.2019.1596899>
- D’Onofre Couto B, Novaes da Costa R, Castro Laurindo W et al (2021) Characterization, techno-functional properties, and encapsulation efficiency of self-assembled β -lactoglobulin nanostructures. *Food Chem* 356:129719. <https://doi.org/10.1016/j.foodchem.2021.129719>
- Delazare T, Ferreira LP, Ribeiro NFP et al (2014) Removal of boron from oilfield wastewater via adsorption with synthetic layered double hydroxides. *J Environ Sci Heal Part A Toxic Hazard Subst Environ Eng* 49:923–932. <https://doi.org/10.1080/10934529.2014.893792>
- Demetriou A, Pashalidis I, Nicolaidis AV, Kumke MU (2013) Surface mechanism of boron on alumina in aqueous solutions. *Desalin Water Treat* 51(31–33):6130–6136. <https://doi.org/10.1080/19443994.2013.764354>

- Demey H, Vincent T, Ruiz M et al (2014) Development of a new chitosan/Ni(OH)₂-based sorbent for boron removal. *Chem Eng J* 244:576–586. <https://doi.org/10.1016/j.cej.2014.01.052>
- Demey H, Barron-Zambrano J, Mhadhbi T et al (2019) Boron removal from aqueous solutions by using a novel alginate-based sorbent: Comparison with Al₂O₃ particles. *Polymers (basel)*. <https://doi.org/10.3390/polym11091509>
- Dolati M, Aghapour AA, Khorsandi H, Karimzade S (2017) Boron removal from aqueous solutions by electrocoagulation at low concentrations. *J Environ Chem Eng* 5:5150–5156. <https://doi.org/10.1016/j.jece.2017.09.055>
- El-Refaey AA, Mahmoud AH, Saleh ME (2015) Bone biochar as a renewable and efficient P fertilizer: a comparative study. *Alex J Agric Res* 60:127–137
- EU (1998) European Council Directive, Directive no. 98/83/EC on the quality of water intended for human consumption. *Off J Eur Communities L* 330 32–54
- Flores-Cano JV, Leyva-Ramos R, Carrasco-Marin F et al (2016) Adsorption mechanism of Chromium(III) from water solution on bone char: effect of operating conditions. *Adsorption* 22:297–308. <https://doi.org/10.1007/s10450-016-9771-3>
- Goren AY, Okten HE (2021) Energy production from treatment of industrial wastewater and boron removal in aqueous solutions using microbial desalination cell. *Chemosphere* 285:131370. <https://doi.org/10.1016/j.chemosphere.2021.131370>
- Guan Z, Lv J, Bai P, Guo X (2016) Boron removal from aqueous solutions by adsorption—a review. *Desalination* 383:29–37. <https://doi.org/10.1016/j.desal.2015.12.026>
- Haghi AK, Pogliani L, Castro EA et al (2017) Applied chemistry and chemical engineering, vol 4, 1st edn. Apple Academic Press, New York
- Heredia AC, De La Fuente García-Soto MM, Narros Sierra A et al (2019) Boron removal from aqueous solutions by synthetic MgAlFe mixed oxides. *Ind Eng Chem Res* 58:9931–9939. <https://doi.org/10.1021/acs.iecr.9b02259>
- Hernández-Hernández LE, Bonilla-Petriciolet A, Mendoza-Castillo DI, Reynel-Ávila HE (2017) Antagonistic binary adsorption of heavy metals using stratified bone char columns. *J Mol Liq* 241:334–346. <https://doi.org/10.1016/j.molliq.2017.05.148>
- Ip AWM, Barford JP, McKay G (2010) A comparative study on the kinetics and mechanisms of removal of reactive black 5 by adsorption onto activated carbons and bone char. *Chem Eng J* 157:434–442. <https://doi.org/10.1016/j.cej.2009.12.003>
- Isaacs-Paez ED, Leyva-Ramos R, Jacobo-Azuara A et al (2014) Adsorption of boron on calcined AlMg layered double hydroxide from aqueous solutions. Mechanism and effect of operating conditions. *Chem Eng J* 245:248–257. <https://doi.org/10.1016/j.cej.2014.02.031>
- Jalali M, Rajabi F, Ranjbar F (2016) The removal of boron from aqueous solutions using natural and chemically modified sorbents. *Desalin Water Treat* 57:8278–8288. <https://doi.org/10.1080/19443994.2015.1020509>
- Jaouadi M (2021) Characterization of activated carbon, wood sawdust and their application for boron adsorption from water. *Int Wood Prod J* 12:22–33. <https://doi.org/10.1080/20426445.2020.1785605>
- Jia P, Tan H, Liu K, Gao W (2017) Enhanced photocatalytic performance of ZnO/bone char composites. *Mater Lett* 205:233–235. <https://doi.org/10.1016/j.matlet.2017.06.099>
- Kabay N, Bryjak M, Hilal N (2015) Boron separation processes, 1st edn. Elsevier, Amsterdam
- Kameda T, Oba J, Yoshioka T (2017) Removal of boron and fluoride in wastewater using Mg–Al layered double hydroxide and Mg–Al oxide. *J Environ Manag* 188:58–63. <https://doi.org/10.1016/j.jenvman.2016.11.057>
- Karahan S, Yurdaoç M, Seki Y, Yurdaoç K (2006) Removal of boron from aqueous solution by clays and modified clays. *J Colloid Interface Sci* 293:36–42. <https://doi.org/10.1016/j.jcis.2005.06.048>
- Kehal M, Reinert L, Duclaux L (2010) Characterization and boron adsorption capacity of vermiculite modified by thermal shock or H₂O₂ reaction and/or sonication. *Appl Clay Sci* 48:561–568. <https://doi.org/10.1016/j.clay.2010.03.004>
- Lin J-Y, Mahasti NNN, Huang Y-H (2021) Recent advances in adsorption and coagulation for boron removal from wastewater: a comprehensive review. *J Hazard Mater* 407:124401. <https://doi.org/10.1016/j.jhazmat.2020.124401>
- Lyu J, Zhang N, Liu H et al (2017) Adsorptive removal of boron by zeolitic imidazolate framework: kinetics, isotherms, thermodynamics, mechanism and recycling. *Sep Purif Technol* 187:67–75. <https://doi.org/10.1016/j.seppur.2017.05.059>
- Medellin-Castillo NA, Padilla-Ortega E, Tovar-García LD et al (2016) Removal of fluoride from aqueous solution using acid and thermally treated bone char. *Adsorption* 22:951–961. <https://doi.org/10.1007/s10450-016-9802-0>
- Meili L, Lins PV, Zanta CLPS et al (2018) Applied clay science MgAl-LDH/biochar composites for methylene blue removal by adsorption. *Appl Clay Sci* 168:11–20. <https://doi.org/10.1016/j.clay.2018.10.012>
- Meili L, Lins PV, Zanta CLPS et al (2019) MgAl-LDH/biochar composites for methylene blue removal by adsorption. *Appl Clay Sci* 168:11–20. <https://doi.org/10.1016/j.clay.2018.10.012>
- Melliti A, Kheriji J, Bessaies H, Hamrouni B (2020) Boron removal from water by adsorption onto activated carbon prepared from palm bark: kinetic, isotherms, optimisation and breakthrough curves modeling. *Water Sci Technol* 81:321–332. <https://doi.org/10.2166/wst.2020.107>
- Mendes KF, de Sousa RN, Takeshita V et al (2019) Cow bone char as a sorbent to increase sorption and decrease mobility of hexazinone, metribuzin, and quinclorac in soil. *Geoderma* 343:40–49. <https://doi.org/10.1016/j.geoderma.2019.02.009>
- Mesquita PL, Cruz MAP, Souza CR et al (2017a) Removal of refractory organics from saline concentrate produced by electro dialysis in petroleum industry using bone char. *Adsorption* 23:983–997. <https://doi.org/10.1007/s10450-017-9917-y>
- Mesquita PL, Souza CR, Santos NTG, Rocha SDF (2017b) Fixed-bed study for bone char adsorptive removal of refractory organics from electro dialysis concentrate produced by petroleum refinery. *Environ Technol* 39:1544–1556. <https://doi.org/10.1080/09593330.2017.1332691>
- Mesquita PL, Mihara HY, Rocha SDF (2018) Regeneração a vapor de carvão de ossos bovinos usado como adsorvente para remoção de orgânicos refratários de concentrado salino do tratamento de efluentes da indústria de petróleo. In: 12^o Encontro Brasileiro sobre Adsorção. Gramado-RS
- Naves FL, Balestrassi PP, Sawhney RS et al (2016) Multivariate normal boundary intersection based on rotated factor scores: a multiobjective optimization method for methyl orange treatment. *J Clean Prod* 143:413–439. <https://doi.org/10.1016/j.jclepro.2016.12.092>
- Nigri EM, Bhatnagar A, Rocha SDF (2016a) Thermal regeneration process of bone char used in the fluoride removal from aqueous solution. *J Clean Prod* 142:3558–3570. <https://doi.org/10.1016/j.jclepro.2016.10.112>
- Nigri EM, Cechinel MAP, Mayer DA et al (2016b) Cow bones char as a green sorbent for fluorides removal from aqueous solutions: batch and fixed-bed studies. *Environ Sci Pollut Res* 24:2364–2380. <https://doi.org/10.1007/s11356-016-7816-5>
- Nigri EM, Santos ALA, Mesquita PL et al (2019) Simultaneous removal of strontium and refractory organic compounds from



- electrodialysis effluents by modified bovine bone char. *Desalin Water Treat* 145:189–201. <https://doi.org/10.5004/dwt.2019.23655>
- Oladipo AA, Gazi M (2016) Efficient boron abstraction using honeycomb-like porous magnetic hybrids: assessment of techno-economic recovery of boric acid. *J Environ Manag* 183:917–924. <https://doi.org/10.1016/j.jenvman.2016.09.059>
- Paixão K, Abreu E, Lamas Samanamud GR et al (2019) Normal boundary intersection applied in the scale-up for the treatment process of eriochrome black T through the UV/TiO₂/O₃ system. *J Environ Chem Eng* 7:102801. <https://doi.org/10.1016/j.jece.2018.11.045>
- Patel S, Han J, Qiu W, Gao W (2015) Journal of environmental chemical engineering synthesis and characterisation of mesoporous bone char obtained by pyrolysis of animal bones, for environmental application. *Biochem Pharmacol* 3:2368–2377. <https://doi.org/10.1016/j.jece.2015.07.031>
- Regalbuto JR, Robles J (2004) The engineering of Pt/carbon catalyst preparation. University of Illinois, Chicago
- Reynel-Avila HE, Mendoza-Castillo DI, Bonilla-Petriciolet A (2016) Relevance of anionic dye properties on water decolorization performance using bone char: adsorption kinetics, isotherms and breakthrough curves. *J Mol Liq* 219:425–434. <https://doi.org/10.1016/j.molliq.2016.03.051>
- Ribeiro MV (2011) Uso de Carvão de Osso Bovino na Defluoretação de Água para Uso em Abastecimento Público. Universidade Federal de Minas Gerais
- Rocha SDF, Ribeiro MV, Viana PR de M, Mansur MB (2011) Bone char: An alternative for the removal of diverse organic and inorganic compounds from industrial wastewaters. In: *Application of adsorbents for water pollution control*. BENTHAM SCIENCE PUBLISHERS, pp 502–522
- Rojas-Mayorga CK, Bonilla-Petriciolet A, Sánchez-Ruiz FJ et al (2015) Breakthrough curve modeling of liquid-phase adsorption of fluoride ions on aluminum-doped bone char using micro-columns: effectiveness of data fitting approaches. *J Mol Liq* 208:114–121. <https://doi.org/10.1016/j.molliq.2015.04.045>
- Saleh M, El-Refaey A, Eldamarawy Y (2020) Effect of bone char application in reducing CO₂ emission and improvement organic matter in calcareous soils. *Egypt J Soil Sci*. <https://doi.org/10.21608/ejss.2020.32612.1363>
- Sasaki K, Toshiyuki K, Ideta K et al (2016) Removal mechanism of high concentration borate by co-precipitation with hydroxyapatite. *J Environ Chem Eng* 4:1092–1101. <https://doi.org/10.1016/j.jece.2016.01.012>
- Simonin JP (2016) On the comparison of pseudo-first order and pseudo-second order rate laws in the modeling of adsorption kinetics. *Chem Eng J* 300:254–263. <https://doi.org/10.1016/j.cej.2016.04.079>
- Thommes M, Kaneko K, Neimark AV et al (2015) Physisorption of gases, with special reference to the evaluation of surface area and pore size distribution (IUPAC Technical Report). *Pure Appl Chem*. <https://doi.org/10.1515/pac-2014-1117>
- Tovar-Gómez R, Moreno-Virgen MR, Dena-Aguilar JA et al (2013) Modeling of fixed-bed adsorption of fluoride on bone char using a hybrid neural network approach. *Chem Eng J* 228:1098–1109. <https://doi.org/10.1016/j.cej.2013.05.080>
- Türker OC, Türe C, Yakar A, Saz Ç (2017) Engineered wetland reactors with different media types to treat drinking water contaminated by boron (B). *J Clean Prod* 168:823–832. <https://doi.org/10.1016/j.jclepro.2017.09.067>
- Wang S, Zhou Y, Gao C (2018) Novel high boron removal polyamide reverse osmosis membranes. *J Memb Sci* 554:244–252. <https://doi.org/10.1016/j.memsci.2018.03.014>
- White RJ, Budarin V, Luque R et al (2009) Tuneable porous carbonaceous materials from renewable resources. *Chem Soc Rev* 38:3401. <https://doi.org/10.1039/b822668g>
- WHO (2017) Guidelines for drinking-water quality: fourth edition incorporating the first addendum. WHO Library Cataloguing-in-Publication Data, Geneva
- Xin J, Huang B (2017) Effects of pH on boron accumulation in cattail (*Typha latifolia*) shoots, and evaluation of floating islands and upward flow mesocosms for the removal of boron from wastewater. *Plant Soil* 412:163–176. <https://doi.org/10.1007/s11104-016-3058-z>
- Yagmur Goren A, Recepoglu YK, Karagunduz A et al (2022) A review of boron removal from aqueous solution using carbon-based materials: an assessment of health risks. *Chemosphere* 293:133587. <https://doi.org/10.1016/j.chemosphere.2022.133587>
- Yan G, Fu L, Lu X et al (2022) Microalgae tolerant of boron stress and bioresources accumulation during the boron removal process. *Environ Res* 208:112639. <https://doi.org/10.1016/j.envres.2021.112639>
- Yang-Zhou C-H, Cao J-X, Dong S-S et al (2021) Phosphorus co-existing in water: a new mechanism to boost boron removal by calcined oyster shell powder. *Molecules* 27:54. <https://doi.org/10.3390/molecules27010054>
- Yoshikawa E, Sasaki A, Endo M (2012) Removal of boron from wastewater by the hydroxyapatite formation reaction using acceleration effect of ammonia. *J Hazard Mater* 237–238:277–282. <https://doi.org/10.1016/j.jhazmat.2012.08.045>
- Zhang X, Wei M, Zhang Z et al (2022) Boron removal by water molecules inside covalent organic framework (COF) multilayers. *Desalination* 526:115548. <https://doi.org/10.1016/j.desal.2022.115548>

Springer Nature or its licensor (e.g. a society or other partner) holds exclusive rights to this article under a publishing agreement with the author(s) or other rightsholder(s); author self-archiving of the accepted manuscript version of this article is solely governed by the terms of such publishing agreement and applicable law.